Cardiac fibrosis in mice lacking brain natriuretic peptide

Naohisa Tamura*, Yoshihiro Ogawa*†, Hideki Chusho*, Kenji Nakamura‡, Kazuki Nakao‡, Michio Suda*, Masato Kasahara*, Ryuju Hashimoto§, Goro Katsuura¶, Masashi Mukoyama*, Hiroshi Itoh*, Yoshihiko Saito*, Issei Tanaka*, Hiroki Otani§, Motoya Katsuki‡, and Kazuwa Nakao*

*Department of Medicine and Clinical Science, Kyoto University Graduate School of Medicine, Kyoto 606-8507, Japan; ‡Laboratory Animal Research Center, Institute of Medical Science, University of Tokyo, Tokyo 108-0071, Japan; §Department of Anatomy, Shimane Medical University, Izumo 693-8501, Japan; and ¶Shionogi Research Laboratories, Shionogi & Co., Ltd., Osaka 553-0002, Japan

Edited by Robert J. Lefkowitz, Duke University Medical Center, Durham, NC, and approved February 1, 2000 (received for review August 31, 1999)

Cardiac fibrosis, defined as a proliferation of interstitial fibroblasts and biosynthesis of extracellular matrix components in the ventricles of the heart, is a consequence of remodeling processes initiated by pathologic events associated with a variety of cardiovascular disorders, which leads to abnormal myocardial stiffness and, ultimately, ventricular dysfunction. Brain natriuretic peptide (BNP) is a cardiac hormone produced primarily by ventricular myocytes, and its plasma concentrations are markedly elevated in patients with congestive heart failure and acute myocardial infarction. However, its precise functional significance has been undefined. In this paper, we report the generation of mice with targeted disruption of BNP (*Nppb*$^{-/-}$ mice). We observed multifocal fibrotic lesions in the ventricles from *Nppb*$^{-/-}$ mice. No signs of systemic hypertension and ventricular hypertrophy are noted in *Nppb*$^{-/-}$ mice. In response to ventricular pressure overload, focal fibrotic lesions are increased in size and number in *Nppb*$^{-/-}$ mice, whereas no focal fibrotic changes are found in wild-type littermates (*Nppb*$^{+/+}$ mice). This study establishes BNP as a cardiomyocyte-derived antifibrotic factor *in vivo* and provides evidence for its role as a local regulator of ventricular remodeling.

In cardiovascular diseases, cardiac overload induces ventricular remodeling, hypertrophy of cardiomyocytes, hyperplasia of fibroblasts, and the accumulation of extracellular matrix components, including collagens, which leads to myocardial fibrosis. Initially, interstitial fibrosis bundles up ventricular myofibers and coordinates force delivery during contraction that opposes increased ventricular load. By contrast, extended fibrosis results in increased myocardial stiffness, causing ventricular dysfunction and, ultimately, heart failure (1). Several lines of evidence suggest that cardiac renin-angiotensin system, endothelin-1, and transforming growth factor (TGF)-β are important local mediators of cardiac fibrosis (1, 2).

The heart is involved in the regulation of blood pressure and fluid-electrolyte balance as an important endocrine organ that secretes two cardiac natriuretic peptides; atrial natriuretic peptide (ANP) and brain natriuretic peptide (BNP) with potent natriuretic, diuretic, and vasorelaxant activities. These peptides are produced by cardiomyocytes and activate a common guanylyl cyclase-coupled natriuretic peptide receptor subtype, guanylyl cyclase-A (GC-A) that is expressed in a wide variety of tissues, thereby leading to an increase in intracellular cGMP concentrations (3–8). It was also demonstrated that the natriuretic peptide/cGMP system might antagonize the proliferation and extracellular matrix production of cardiac fibroblasts through the inhibition of renin-angiotensin and endothelin systems (2, 9, 10). Synthesis and secretion of ANP and BNP are markedly augmented in patients with congestive heart failure and animal models of ventricular hypertrophy (4–6, 11, 12). In addition, plasma BNP concentrations are markedly increased in the early phase of acute myocardial infarction, when plasma ANP concentrations are increased only slightly (13). It is also reported that in patients with congestive heart failure and myocardial infarction, sustained increase in plasma BNP concentrations is correlated with enlargement, decreased contractility, and increased stiffness of the left ventricle (14, 15). These observations suggest that BNP may play important roles in ventricular remodeling. However, the precise functional significance of BNP is not yet understood.

To investigate the physiologic significance of BNP in cardiovascular regulation, we generated *Nppb*$^{-/-}$ mice by gene targeting and analyzed their phenotypes. To further assess the pathophysiologic roles of BNP in ventricular remodeling, we also examined responses of *Nppb*$^{-/-}$ mice to ventricular pressure overload induced by aortic constriction.

Materials and Methods

Gene Targeting. A targeting vector was constructed by replacing exons 1 and 2 of the 129/Sv mouse *Nppb*, which encode the entire coding sequences of mouse BNP except for the C-terminal 5 aa residues, with the neomycin-resistance gene (Fig. 1*A*). The targeting vector was introduced into embryonic stem cells by electroporation (16). Double selection in G418 and ganciclovir produced seven homologous recombinant embryonic stem cell clones that were analyzed by Southern blot analysis using the 5′ and 3′ external probes indicated (Fig. 1 *A* and *B*). Male chimeras derived from three independent clones with germ-line transmission of the disrupted allele were bred to C57BL/6J or 129/SvJ females. The care of the animals and all experiments were conducted in accordance with the institutional guideline of Kyoto University Graduate School of Medicine.

RNA and Peptide Analysis. Total RNA was extracted from mouse tissues. Northern blot analysis was performed using the mouse ANP (*Nppa*), *Nppb* (17), rat TGF-β_1 [63197; American Type Culture Collection (ATCC)], human TGF-β_3 (63199; ATCC), rat endothelin-1 (18), rat sarcoplasmic reticulum Ca^{2+}-ATPase (a gift from Larry Kedes, University of Southern California, Los Angeles), human pro-α_1 (I) collagen (61323; ATCC), and human glyceraldehyde-3-phosphate dehydrogenase (57091; ATCC) cDNA fragments, and a mouse skeletal α-actin (*Acta1*)-specific antisense oligonucleotide (5′-CGATTGTCGATTGTGGTCCTGAGGAGAGAGAGCGCGAACGCAGACGCGAGTCGCCT-3′) as probes. Angiotensin-converting enzyme (*Ace)* mRNA expression

This paper was submitted directly (Track II) to the PNAS office.

Abbreviations: BNP, brain natriuretic peptide; ANP, atrial natriuretic peptide; TGF, transforming growth factor; ACE, angiotensin-converting enzyme; RT-PCR, reverse transcription–PCR; GC-A, guanylyl cyclase-A.

†To whom reprint requests should be addressed at: Department of Medicine and Clinical Science, Kyoto University Graduate School of Medicine, 54 Shogoin Kawahara-cho, Sakyo-ku, Kyoto 606-8507, Japan. E-mail:ogawa@kuhp.kyoto-u.ac.jp.

The publication costs of this article were defrayed in part by page charge payment. This article must therefore be hereby marked "*advertisement*" in accordance with 18 U.S.C. §1734 solely to indicate this fact.

Article published online before print: *Proc. Natl. Acad. Sci. USA*, 10.1073/pnas.070371497. Article and publication date are at www.pnas.org/cgi/doi/10.1073/pnas.070371497

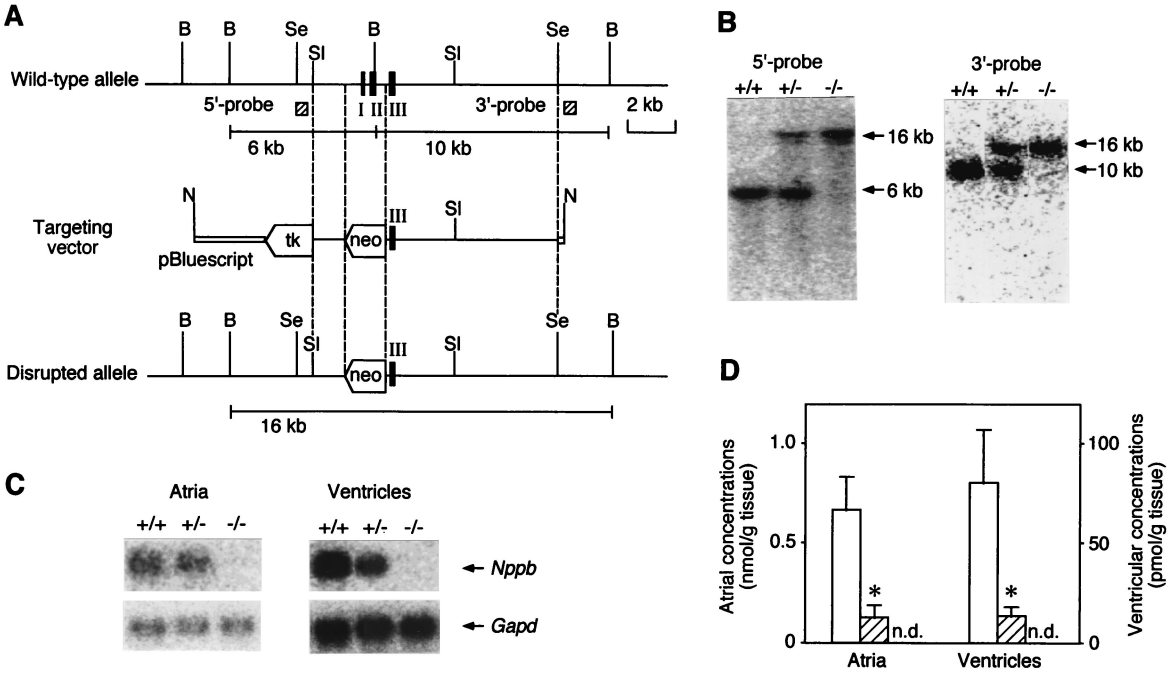

Fig. 1. Targeted disruption of *Nppb*. (*A*) Restriction maps of the wild-type 129/Sv mouse *Nppb* allele, targeting vector, and predicted disrupted allele. Filled bars indicate exons (I–III). The genomic fragments used as 5′ and 3′ external probes are shown as hatched boxes. B, *Bam*HI; Se, *Spe*I; Sl, *Sal*I; N, *Not*I; tk, herpes simplex virus thymidine kinase gene; neo, neomycin-resistance gene. (*B*) Southern blot analysis of genomic DNAs from F_2 offspring generated by heterozygous intercrosses of F_1 mice upon digestion with *Bam*HI. (*C*) Northern blot analysis of *Nppb* mRNA in atria and ventricles from $Nppb^{+/+}$, $Nppb^{+/-}$, and $Nppb^{-/-}$ mice. Total RNAs (1 and 10 μg) from atria and ventricles, respectively, were analyzed. (*D*) Cardiac BNP concentrations in $Nppb^{+/+}$, $Nppb^{+/-}$, and $Nppb^{-/-}$ mice ($n = 3$). Open and hatched bars represent $Nppb^{+/+}$ and $Nppb^{+/-}$ mice, respectively. n.d., not detectable in $Nppb^{-/-}$ mice. *, $P < 0.05$ vs. $Nppb^{+/+}$ mice.

was assessed by reverse transcription–PCR (RT-PCR) analysis (sense primer, 5′-CACTACACCAGTGTGACATCTACC-3′; antisense primer, 5′-GATGTGGCCATC-ATGTTTGTTAGA-3′), followed by Southern blot analysis with an *Ace*-specific sense oligonucleotide probe (5′-AGTACAACCAGATCCTGCTA-3′). Total RNA (2 μg) was reverse transcribed by an oligo(dT) primer, and one-tenth of the reaction was subjected to the PCR. As an internal control, RT-PCR and Southern blot analysis for mouse glyceraldehyde-3-phosphate dehydrogenase (*Gapd*) mRNA was also performed (sense and antisense primers and a mouse glyceraldehyde-3-phosphate dehydrogenase control amplimer set, CLONTECH; antisense probe, 5′-GCCTTGACTGTGCCGTTGAATTTGCCGTGA-3′). We have confirmed that the intensity of hybridization signals shows a linear relation with the amount of total RNAs used in Northern blot analysis, RT-PCR, and Southern blot analysis. The hybridization signal intensity was quantitated by using an image analyzer BAS-2500 (Fuji) and normalized for the *Gapd* mRNA signal intensity. ANP and BNP concentrations were determined by the RIAs specific for ANP and mouse BNP, respectively (17).

Blood Pressure Measurement. Twenty-week-old male mice were fed on a standard-salt (0.7% NaCl) or a high-salt (8.0% NaCl) diet for 4 wk. Blood pressure and pulse rate were measured by the tail-cuff method (17). After 7 days of training, at least 10 readings were taken for each measurement.

Blood and Urinary Parameter Measurements. Plasma aldosterone concentrations were determined by using a human aldosterone RIA kit (Dainabot, Tokyo). A commercially available RIA (Yamasa Shoyu, Tokyo) determined plasma concentrations and urinary excretion of cGMP. Mice were placed in metabolic cages that provided free access to tap water and food. Daily urine volume and urinary Na^+ and K^+ excretion were measured after the animals were fed for 4 wk on either the standard-salt diet or the high-salt diet.

Histology. For light microscopy, tissues were fixed in Carnoy's solution and embedded in paraffin. Sections (2 μm thick) were cut from paraffin-embedded specimens and stained with hematoxylin and eosin or Masson's trichrome stainings. Cardiac fibrosis areas (both perivascular and focal fibrosis areas) were measured by a light microscope equipped with an image analyzing system (KS 400 Imaging System; Carl Zeiss Vision, Eching, Germany). In ventricles from 20-wk-old $Nppb^{+/+}$ and $Nppb^{-/-}$ mice, which were fixed in 4% paraformaldehyde in 0.1 M phosphate buffer (pH 7.4), TGF-β_3 protein levels were assessed by immunohistochemical analysis (19). For transmission electron microscopy, cardiac tissues were fixed in 4% paraformaldehyde and 0.5% glutaraldehyde in 0.1 M phosphate buffer (pH 7.4) and postfixed in 1% aqueous osmium tetroxide. The specimens were dehydrated in a graded series of ethanol and embedded in epoxy resin (TAAB 812). Ultrathin sections were cut at 70 nm, stained with uranyl acetate and lead citrate, and examined with an electron microscope (002B; Topcon Technologies, Paramus, NJ) at 80 kV. To reduce the potential observer bias, samples always were examined and photographed by the same individual (R.H.) without the individual being informed of the genotype of each sample.

Aortic Constriction. Twenty-week-old male mice were anesthetized by i.p. injection of pentobarbital (50 mg/kg of body weight), and suprarenal abdominal aorta was ligated by 7-0 nylon suture against a 27-gauge needle (20). The tail-cuff systolic blood pressure was reduced by 30–40 mmHg (1 mmHg = 133 Pa) in $Nppb^{+/+}$ and $Nppb^{-/-}$ mice by the abdominal aortic constriction. The sham-operated animals underwent identical surgical procedures, except that the ligation of aorta was not performed.

Mice were killed, and cardiac tissues were removed 7 days after the surgery.

Statistical Analysis. Data are expressed as group means ± SE. Comparison among genotypes was assessed by analysis of variance (ANOVA) and completed by Fisher's probable least significant difference test as required. Comparison among genotypes and treatments was assessed by two-way ANOVA. If there was significant interaction between genotypes and treatments, one-way ANOVA was performed among all groups.

Results and Discussion

Generation of *Nppb*$^{-/-}$ Mice. To investigate the physiologic and pathophysiologic roles of BNP *in vivo*, we generated mice with a disrupted *Nppb* allele by gene targeting in 129/Sv mouse-derived embryonic stem cells (Fig. 1*A*). Male chimeras with germ-line transmission of the disrupted allele were bred to C57BL/6J and 129/SvJ females (Fig. 1*B*). Analysis of 25 intercrosses between mice heterozygous for the disrupted allele on a pure 129/Sv background revealed that the genotype ratio of +/+:+/−:−/− at weaning is 1.0:2.0:1.0 ($n = 196$), conforming to the expected Mendelian proportions.

Northern blot analysis revealed that *Nppb* mRNA levels are decreased ≈50% in atria and ventricles from *Nppb*$^{+/-}$ mice as compared with *Nppb*$^{+/+}$ mice (Fig. 1*C*). BNP concentrations in atria and ventricles from *Nppb*$^{+/-}$ mice also were decreased relative to those found in *Nppb*$^{+/+}$ mice ($P < 0.05$ by unpaired Student's t test) (Fig. 1*D*). No *Nppb* transcript and BNP were detected in cardiac tissues from *Nppb*$^{-/-}$ mice (Fig. 1 *C* and *D*). All of the data indicate that disruption of the *Nppb* allele results in complete loss of *Nppb* mRNA and BNP. *Nppb*$^{-/-}$ mice were viable throughout adulthood, and both sexes were fertile. No gross skeletal abnormalities were noted in *Nppb*$^{-/-}$ mice, although transgenic mice overexpressing *Nppb* have been shown to exhibit marked skeletal overgrowth accompanied by increased endochondral ossification (21). This is consistent with the notion that C-type natriuretic peptide, a third natriuretic peptide, is an endogenous ligand involved in endochondral ossification (22).

Blood Pressure and Fluid-Electrolyte Balance. The tail-cuff systolic blood pressure of *Nppb*$^{-/-}$ mice did not differ significantly from those of *Nppb*$^{+/+}$ and *Nppb*$^{+/-}$ mice on the standard-salt diet (+/+, 121 ± 2 mmHg; +/−, 116 ± 2 mmHg; −/−, 118 ± 3 mmHg; $n = 8$) or high-salt diet (+/+, 118 ± 5 mmHg; +/−, 116 ± 3 mmHg; −/−, 117 ± 4 mmHg; $n = 8$). No significant differences were noted among three genotypes on the standard-salt diet or on the high-salt diet in pulse rate, hematocrit, serum Na^+ and K^+ concentrations, plasma aldosterone concentration, urine volume, and urinary Na^+ and K^+ excretion (data not shown). There were also no significant differences in plasma concentrations and urinary excretion of cGMP between *Nppb*$^{-/-}$ and *Nppb*$^{+/+}$ mice (data not shown). No appreciable differences in the above parameters were noted among genotypes on both 129/B_6 hybrid and pure 129/Sv backgrounds. These results indicate that BNP is not involved in the regulation of blood pressure and fluid-electrolyte balance under physiologic conditions. However, transgenic mice overexpressing *Nppb* exhibit an observable reduction in blood pressure (17), suggesting that BNP participates in the regulation of blood pressure when it circulates in a large quantity in cardiovascular disorders (4, 5, 13).

Cardiac Phenotypes of *Nppb*$^{-/-}$ Mice. We also analyzed cardiac histology and mRNA expression in mice having a pure 129/Sv background. Hearts from *Nppb*$^{+/+}$ and *Nppb*$^{-/-}$ mice had similar gross anatomy. Heart-to-body weight ratios of *Nppb*$^{-/-}$ mice were not significantly different from those of *Nppb*$^{+/+}$ mice (+/+, 4.8 ± 0.1 mg/g; −/−, 4.8 ± 0.1 mg/g in 20-wk-old males; $n = 10$). Nevertheless, histologic examinations revealed multifocal fibrotic lesions in subendocardial regions of ventricles from male *Nppb*$^{-/-}$ mice at 15 wk of age and thereafter (12 of 23 animals examined), whereas no such phenotypes were found in age-matched male *Nppb*$^{+/+}$ mice ($n = 15$) (Fig. 2*A–D*). By contrast, cardiac fibrosis was not found in ventricles from male *Nppb*$^{-/-}$ mice at 5–10 wk of age. We postulate that a variety of cardiac stresses such as a transient elevation in blood pressure and heart rate may increase the rate and severity of cardiac fibrosis in *Nppb*$^{-/-}$ mice as they age. In this study, the degree of cardiac fibrosis was lower in female *Nppb*$^{-/-}$ mice than in males at 20 wk of age. Histology of the cerebrum, cerebellum, lung, aorta, kidney, liver, spleen, intestine, colon, testis, and bone was unremarkable.

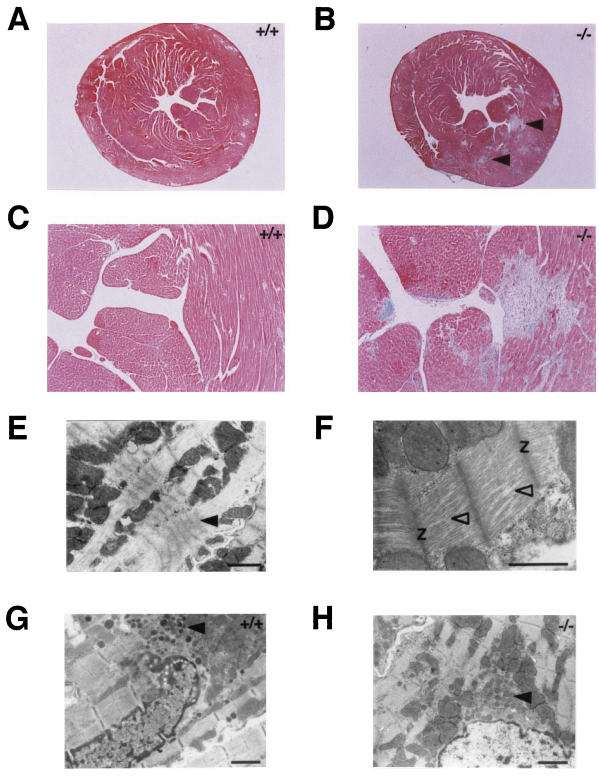

Fig. 2. Light and electron microscopic examinations of hearts from *Nppb*$^{+/+}$ and *Nppb*$^{-/-}$ mice. (*A* and *B*) Masson's trichrome staining of transverse sections of ventricles from *Nppb*$^{+/+}$ (*A*) and *Nppb*$^{-/-}$ (*B*) mice at the level of papillary muscles. Focal fibrotic lesions are indicated by arrowheads. (*C* and *D*) Higher magnification (×25) of subendocardial regions of ventricles from *Nppb*$^{+/+}$ (*C*) and *Nppb*$^{-/-}$ (*D*) mice. (*E* and *F*) Electron microscopy of left ventricular free wall from *Nppb*$^{-/-}$ mice. Supercontracted sarcomeres and disorganized myofibrils are indicated by filled and open arrowheads, respectively. Z, Z-bands in sarcomeres. (*G* and *H*) Electron microscopy of atria from *Nppb*$^{+/+}$ (*G*) and *Nppb*$^{-/-}$ (*H*) mice. Atrial granules are indicated by arrowheads. (Scale bars represent 1 μm in *E–H*.)

We also examined by transmission electron microscopy the ultrastructure of ventricular cardiocyte myofibers. In *Nppb*$^{+/+}$ mice, myofibrils were well organized in parallel arrays. In contrast, supercontracted sarcomeres and disorganized myofibrils were observed in some ventricular myocytes from *Nppb*$^{-/-}$ mice of 6–30 wk of age (Fig. 2 *E* and *F*). The ultrastructural defects similar to those found in *Nppb*$^{-/-}$ mice are often observed in ventricles from BIO14.6 cardiomyopathic hamsters by 6–10 wk of age, when they exhibit small areas of myolysis and fibrotic lesions with no overt cardiac dysfunction (23). Because such ultrastructural defects precede the myolysis and cardiac fibrosis in BIO14.6 cardiomyopathic hamsters, it is conceivable that supercontraction and disorganization of sarcomeres are

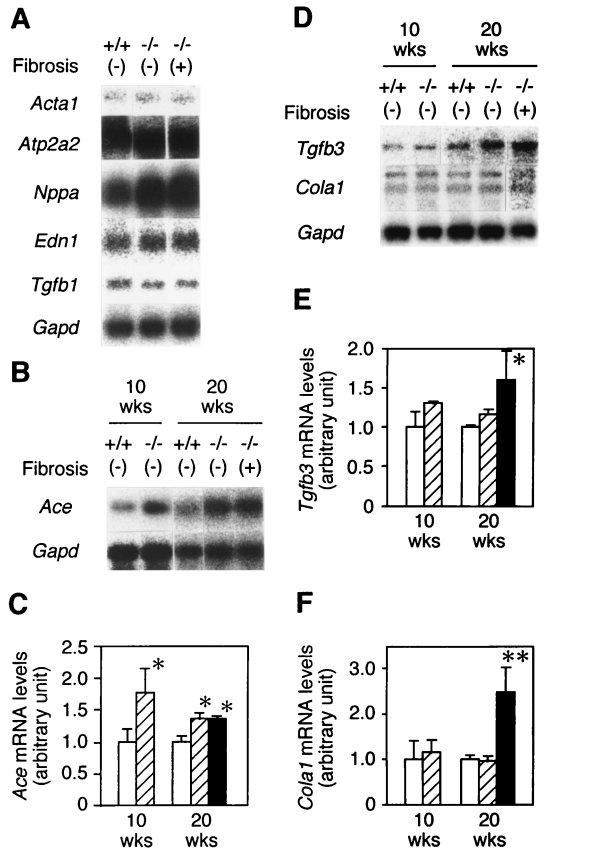

Fig. 3. Gene expression in ventricles from $Nppb^{+/+}$ and $Nppb^{-/-}$ mice. (*A*) Northern blot analysis of *Acta1*, *Atp2a2*, *Nppa*, *Edn1*, and *Tgfb1* mRNAs in ventricles from $Nppb^{+/+}$ mice ($n = 10$) and $Nppb^{-/-}$ mice with or without cardiac fibrosis ($n = 5$ for each) at 20 wk of age. Hybridization signal for *Gapd* mRNA was used as an internal control. Total RNAs (20 μg) were analyzed, and representative cases are presented. (*B–F*) Shown are RT-PCR and Southern blot analysis of *Ace* mRNA (*B* and *C*) and Northern blot analysis of *Tgfb3* and *Cola1* mRNAs (*D–F*) in ventricles from $Nppb^{+/+}$ and $Nppb^{-/-}$ mice at 10 wk of age ($n = 5$ for each) and ventricles from $Nppb^{+/+}$ mice ($n = 15$) and $Nppb^{-/-}$ mice with or without cardiac fibrosis ($n = 8$ for each) at 20 wk of age. Representative cases (*B* and *D*) and quantification of *Ace* (*C*), *Tgfb3* (*E*), and *Cola1* (*F*) mRNA levels are shown. Open, hatched, and filled bars represent mRNA levels for $Nppb^{+/+}$ mice, $Nppb^{-/-}$ mice without cardiac fibrosis, and $Nppb^{-/-}$ mice with cardiac fibrosis, respectively. The mean mRNA levels in $Nppb^{+/+}$ mice (open bars) were defined as 1.0 arbitrary unit. *, $P < 0.05$; **, $P < 0.01$ vs. $Nppb^{+/+}$ mice.

caused by the lack of BNP, which may precede cardiac fibrosis in $Nppb^{-/-}$ mice. Atrial sections from $Nppb^{-/-}$ mice also were analyzed by transmission electron microscopy, because $Nppa^{-/-}$ mice have no detectable atrial granules (24). Unlike $Nppa^{-/-}$ mice, $Nppb^{-/-}$ mice had atrial granules (Fig. 2 *G* and *H*).

Cardiac mRNA Expression in $Nppb^{-/-}$ Mice. We examined expression of mRNAs for *Acta1* and sarcoplasmic reticulum Ca^{2+}-ATPase (*Atp2a2*), markers of ventricular hypertrophy (11), in ventricles from 20-wk-old $Nppb^{-/-}$ mice with or without cardiac fibrosis. No significant differences in *Acta1* and *Atp2a2* mRNA levels were noted between $Nppb^{+/+}$ and $Nppb^{-/-}$ mice (Fig. 3*A*), which is consistent with no apparent ventricular hypertrophy in $Nppb^{-/-}$ mice. By contrast, *Nppa* mRNA expression was markedly increased in ventricles from 20-wk-old $Nppb^{-/-}$ mice relative to $Nppb^{+/+}$ mice (Fig. 3*A*). Ventricular ANP concentrations were also increased in $Nppb^{-/-}$ mice as compared with $Nppb^{+/+}$ mice (+/+, 8 ± 5; −/−, 296 ± 61 pmol/g of tissue; $P < 0.01$; $n = 4$). Increase in ventricular *Nppa* mRNA and ANP may be a consequence of the above ultrastructural defects and cardiac fibrosis (25). No significant differences in atrial *Nppa* mRNA and ANP were noted between the genotypes. Plasma ANP concentrations were unchanged in $Nppb^{-/-}$ mice as compared with $Nppb^{+/+}$ mice (data not shown), which is consistent with the concept that the circulating ANP is derived mainly from the atrium (7). We also examined expression of TGF-β_1 (*Tgfb1*), TGF-β_3 (*Tgfb3*), endothelin-1 (*Edn1*), and *Ace* mRNAs, which are shown to be involved in cardiac fibroblast proliferation and biosynthesis of extracellular matrix proteins such as pro-α_1 (I) collagen (1, 2). Expression of *Edn1* and *Tgfb1* mRNAs were unchanged in 20-wk-old $Nppb^{-/-}$ mice with or without cardiac fibrosis as compared with $Nppb^{+/+}$ mice (Fig. 3*A*). However, in 20-wk-old $Nppb^{-/-}$ mice without cardiac fibrosis, *Ace* mRNA expression was increased relative to $Nppb^{+/+}$ mice (≈1.5-fold) (Fig. 3 *B* and *C*). Expression of *Tgfb3* mRNA tended to be increased, although not statistically significantly (Fig. 3 *D* and *E*). In 20-wk-old $Nppb^{-/-}$ mice with cardiac fibrosis, *Ace* and *Tgfb3* mRNA levels were increased relative to those in $Nppb^{+/+}$ mice (≈1.5-fold) (Fig. 3 *B–E*). Expression of pro-α_1 (I) collagen (*Cola1*) mRNA was increased in 20-wk-old $Nppb^{-/-}$ mice with cardiac fibrosis (≈2.5-fold relative to $Nppb^{+/+}$ mice) but not in those without cardiac fibrosis (Fig. 3 *D* and *F*). The pattern of cardiac mRNA expression in 20-wk-old $Nppb^{-/-}$ mice with cardiac fibrosis is similar to that found in mice with targeted disruption of the GC-A gene ($Npr1^{-/-}$ mice) (ref. 26 and N.T., Y.O., H.C., D. L. Garbers, and K. Nakao, unpublished data). At 10 wk of age, when no cardiac fibrosis occurred in ventricles from $Nppb^{-/-}$ mice, *Ace* mRNA levels also were increased significantly in $Nppb^{-/-}$ mice relative to $Nppb^{+/+}$ mice (≈2-fold) (Fig. 3 *B* and *C*). *Tgfb3* mRNA levels tended to increase, although not statistically significantly (Fig. 3 *D* and *E*). No significant changes in *Cola1* mRNA levels were noted between $Nppb^{-/-}$ and $Nppb^{+/+}$ mice (Fig. 3 *D* and *F*). Immunohistochemical analysis revealed that TGF-β_3 protein levels have increased in ventricles from 20-wk-old $Nppb^{-/-}$ mice with cardiac fibrosis (data not shown). Cardiac ACE protein levels and/or ACE activities are reported to be roughly parallel to *Ace* mRNA expression (27, 28), suggesting that the ACE activity is also increased in ventricles from $Nppb^{-/-}$ mice. Increased ACE and TGF-β_3 should stimulate collagen production and cardiac fibrosis. Therefore, BNP might prevent the development of cardiac fibrosis through the inhibition of cardiac ACE and TGF-β_3 production. This finding is consistent with a previous *in vitro* observation that natriuretic peptides antagonize the growth factor-induced proliferation of cardiac fibroblasts, where natriuretic peptide receptors are expressed abundantly (9).

Exaggerated Cardiac Fibrosis in Response to Ventricular Pressure Overload in $Nppb^{-/-}$ Mice. We also examined responses of $Nppb^{-/-}$ mice to ventricular pressure overload induced by aortic constriction (20). At 7 days after the surgery, the heart-to-body weight ratios were increased significantly in both $Nppb^{+/+}$ and $Nppb^{-/-}$ mice as compared with sham-operated controls, whereas no significant differences were noted between the genotypes (+/+, constricted, 5.2 ± 0.1 mg/g; sham-operated, 4.6 ± 0.1 mg/g; −/−, constricted, 5.2 ± 0.5 mg/g; sham-operated, 4.5 ± 0.1 mg/g; constricted vs. sham-operated, $P < 0.05$; +/+ vs. −/−, not significant; $n = 7$). These data suggest that the strength of aortic constriction-induced pressure overload was similar in both genotypes. In this study, in response to the ventricular pressure overload, no focal fibrotic lesions were found in $Nppb^{+/+}$ mice (Fig. 4*A*). By contrast, multifocal fibrotic lesions were increased in size and number in ventricles from $Nppb^{-/-}$ mice after the aortic constriction (Fig. 4*B*). Fibrosis to total area ratios were increased significantly only in $Nppb^{-/-}$ mice after the aortic constriction (≈3-fold relative to sham-operated $Nppb^{-/-}$ mice) (Fig. 4*C*). In response to the ventricular pressure overload, *Nppb* mRNA expression was markedly increased in ventricles from $Nppb^{+/+}$ mice (Fig. 4*D*). After the

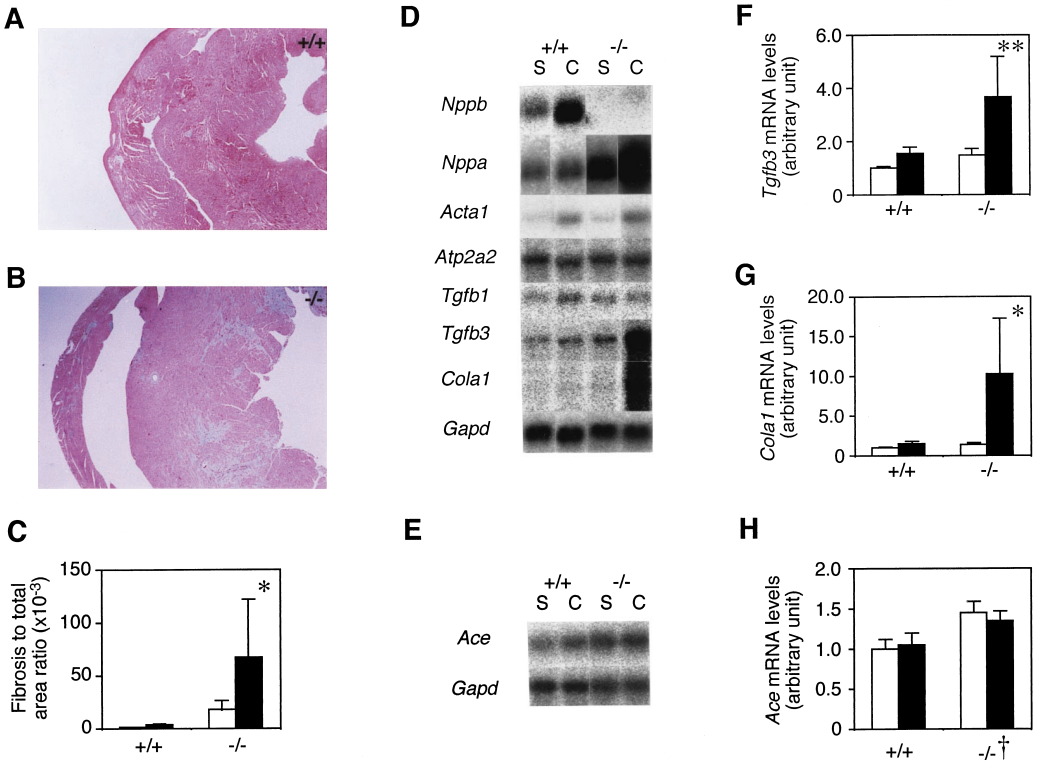

Fig. 4. Cardiac fibrosis and cardiac gene expression in $Nppb^{+/+}$ and $Nppb^{-/-}$ mice that received abdominal aortic constriction. (*A* and *B*) Masson's trichrome staining of transverse sections of ventricles from $Nppb^{+/+}$ (*A*) and $Nppb^{-/-}$ (*B*) mice at the level of papillary muscles 7 days after aortic constriction. (*C*) Fibrosis-to-total area ratios of ventricular transverse sections from $Nppb^{+/+}$ and $Nppb^{-/-}$ mice that received sham operation (open bars) or aortic constriction (filled bars) ($n = 7$). *, $P < 0.05$ vs. sham-operated group by one-way ANOVA among four groups. (*D*) Northern blot analysis of *Nppb*, *Nppa*, *Acta1*, *Atp2a2*, *Tgfb1*, *Tgfb3*, and *Cola1* mRNAs. Total RNAs (10 μg) were used in each lane. S, sham-operated; C, constricted. (*E*) RT-PCR and Southern blot analysis of *Ace* mRNA are shown. (*F–H*) Quantification of *Tgfb3* (*F*), *Cola1* (*G*), and *Ace* (*H*) mRNA levels in ventricles from sham-operated (open bars) and constricted (closed bars) mice of each genotype ($n = 7$). The mean mRNA level for each gene in sham-operated $Nppb^{+/+}$ mice was defined as 1.0 arbitrary unit. *, $P < 0.05$; **, $P < 0.01$ vs. sham-operated mice by one-way ANOVA among four groups (*F* and *G*). †, $P < 0.05$ vs. $Nppb^{+/+}$ mice by two-way ANOVA (*H*).

aortic constriction, *Nppa* and *Acta1* mRNA levels were increased, whereas *Atp2a2* mRNA levels were decreased in ventricles from both $Nppb^{+/+}$ and $Nppb^{-/-}$ mice (Fig. 4*D*), which is consistent with the development of ventricular hypertrophy in both genotypes. No significant changes in *Tgfb1* mRNA levels were noted in ventricles from $Nppb^{+/+}$ and $Nppb^{-/-}$ mice treated with the aortic constriction. In response to the ventricular pressure overload, *Tgfb3* and *Cola1* mRNA levels were increased in ventricles from $Nppb^{-/-}$ mice (≈4- and 10-fold increases, respectively, relative to sham-operated $Nppb^{-/-}$ mice), although unchanged in $Nppb^{+/+}$ mice (Fig. 4 *D*, *F*, and *G*). When treated with the aortic constriction, *Ace* mRNA levels in $Nppb^{-/-}$ mice remained ≈1.5-fold higher than those in $Nppb^{+/+}$ mice, although levels were not increased in either genotype (Fig. 4 *E* and *H*). The mechanism by which BNP modulates cardiac fibrosis is not clear at present. It was reported that nitric oxide, which increases the cGMP production through soluble guanylyl cyclases, inhibits cardiac ACE activity (29), suggesting that cGMP can suppress cardiac ACE activity. In response to various stimuli such as aortic constriction, increased ventricular expression of BNP may lead to a sharp elevation of ventricular cGMP concentrations, thus inhibiting cardiac ACE activity and cardiac fibrosis. Ventricular *Nppb* mRNA and plasma BNP concentrations evidently are elevated in the early phase of acute myocardial infarction (within 24 h after infarction) in rats and humans, when ventricular synthesis and secretion of ANP have not yet been increased (13, 30). In addition, induction of *Nppb* mRNA is turned on and off more rapidly than that of *Nppa* mRNA during the process of ventricular myocyte hypertrophy *in vitro* (31). In the 3′ untranslated region of *Nppb* mRNA, but not of *Nppa* mRNA, there are several copies of the AUUUA motif, which is implicated in mRNA instability (4). All these findings suggest that BNP plays a role different from that of ANP in acute ventricular overload; BNP may act as an "emergency" cardiac hormone to prevent the development of cardiac fibrosis during ventricular pressure overload *in vivo*. In this study, in $Nppb^{-/-}$ mice, ANP alone might not prevent the progression of cardiac fibrosis, possibly because of the slower induction of ANP than that of BNP during ventricular overload (31). However, there is also another possibility, that a receptor specific for BNP may exist in the heart to prevent cardiac fibrosis.

BNP as a Cardiomyocyte-Derived Antifibrotic Factor. Cardiac fibrosis arises from complex interactions between cardiac myocytes and nonmyocytes, in which several locally produced regulatory factors may possibly be involved (1, 2, 18). Our data suggest that BNP constitutes an intracardiac counterregulatory mechanism that prevents the development of cardiac fibrosis *in vivo*; it may serve as a cardiomyocyte-derived antifibrotic signal to cardiac fibroblasts during the process of ventricular remodeling. In this regard, it is interesting to note that glomerular injury and interstitial fibrosis induced by unilateral ureteral obstruction is suppressed significantly in transgenic mice overexpressing BNP in the liver (M. Kasahara, M.M., Y.O., N.T., I.T., and K. Nakao, unpublished data), suggesting that BNP can also act as an antifibrotic factor in other organs through systemic release. The heart produces two cardiac natriuretic peptides, ANP and BNP, both of which are able to activate GC-A with equal potential (8). The $Npr1^{-/-}$ mice show

salt-resistant hypertension and ventricular hypertrophy with cardiac fibrosis (26, 32), whereas *Nppa*$^{-/-}$ mice have salt-sensitive hypertension and ventricular hypertrophy without cardiac fibrosis (24). Our *Nppb*$^{-/-}$ mice exhibit cardiac fibrosis with no signs of hypertension and ventricular hypertrophy. As a result, we postulate that ANP and BNP play complementary roles in the regulation of cardiovascular homeostasis through GC-A. ANP is secreted from the atrium into the circulation in response to atrial stretch (7) and may act as an antihypertensive and antihypervolemic factor by means of GC-A that is expressed in the blood vessel and kidney. Conversely, BNP is produced primarily by the ventricle in response to ventricular overload and may act locally as an antifibrotic factor through GC-A that is expressed in the ventricle.

We thank T. Shiroishi for the 129/SvJ mouse strain; S. Matsuda for blood pressure measurements; K. Katsuki, K. Watanabe, K. Okada, and H. Hiratani for technical assistance; S. Samala for editing the manuscript; and Y. Nakajima, H. Maeda, and Y. Isa for secretarial assistance. This work was supported by grants from the Japanese Ministry of Education, Science, Sports, and Culture; the Japanese Ministry of Health and Welfare; the Yamanouchi Foundation for Research on Metabolic Disorders; the Kanae Foundation for Life and Sociomedical Science; the Salt Science Research Foundation; the Japan Heart Foundation Grant Research on Hypertension and Vascular Metabolism; the Mochida Memorial Foundation for Medical Pharmaceutical Research; the Tanabe Medical Frontier Conference; and ''Research for the Future'' of Japan Society for the Promotion of Science (JSPS-RFTF 96100204 and 98L00801).

1. Weber, K. T. & Brilla, C. G. (1991) *Circulation* **83,** 1849–1865.
2. Butt, R. P., Laurent, G. J. & Bishop, J. E. (1995) *Ann. N.Y. Acad. Sci.* **752,** 387–393.
3. Sudoh, T., Kangawa, K., Minamino, N. & Matsuo, H. (1988) *Nature (London)* **332,** 78–81.
4. Ogawa, Y. & Nakao, K. (1995) in *Hypertension: Pathophysiology, Diagnosis, and Management,* eds. Laragh, J. H. & Brenner, B. M. (Raven, New York), pp. 833–840.
5. Mukoyama, M., Nakao, K., Hosoda, K., Suga, S., Saito, Y., Ogawa, Y., Shirakami, G., Jougasaki, M., Obata, K., Yasue, H., *et al.* (1991) *J. Clin. Invest.* **87,** 1402–1412.
6. Dagnino, L., Drouin, J. & Nemer, M. (1991) *Mol. Endocrinol.* **5,** 1292–1300.
7. De Bold, A. J. (1985) *Science* **230,** 767–770.
8. Chinkers, M. & Garbers, D. L. (1991) *Annu. Rev. Biochem.* **60,** 553–575.
9. Cao, L. & Gardner, D. G. (1995) *Hypertension* **25,** 227–234.
10. Fujisaki, H., Ito, H., Hirata, Y., Tanaka, M., Hata, M., Lin, M., Adachi, S., Akimoto, H., Marumo, F. & Hiroe, M. (1995) *J. Clin. Invest.* **96,** 1059–1065.
11. Izumo, S., Nadal-Ginard, B. & Mahdavi, V. (1988) *Proc. Natl. Acad. Sci. USA* **85,** 339–343.
12. Tamura, N., Ogawa, Y., Itoh, H., Arai, H., Suga, S., Nakagawa, O., Komatsu, Y., Kishimoto, I., Takaya, K., Yoshimasa, T., *et al.* (1994) *J. Clin. Invest.* **94,** 1059–1068.
13. Morita, E., Yasue, H., Yoshimura, M., Ogawa, H., Jougasaki, M., Matsumura, T., Mukoyama, M., Nakao, K. & Imura, H. (1993) *Circulation* **88,** 82–91.
14. Yamamoto, K., Burnett, J. C., Jr., Jougasaki, M., Nishimura, R. A., Bailey, K. R., Saito, Y., Nakao, K. & Redfield, M. M. (1996) *Hypertension* **28,** 988–994.
15. Nagaya, N., Goto, Y., Nishikimi, T., Uematsu, M., Miyao, Y., Kobayashi, Y., Miyazaki, S., Hamada, S., Kuribayashi, S., Takamiya, M., *et al.* (1999) *Clin. Sci.* **96,** 129–136.
16. Gondo, Y., Nakamura, K., Nakao, K., Sasaoka, T., Ito, K., Kimura, M. & Katsuki, M. (1994) *Biochem. Biophys. Res. Commun.* **202,** 830–837.
17. Ogawa, Y., Itoh, H., Tamura, N., Suga, S., Yoshimasa, T., Uehira, M., Matsuda, S., Shiono, S., Nishimoto, H. & Nakao, K. (1994) *J. Clin. Invest.* **93,** 1911–1921.
18. Harada, M., Itoh, H., Nakagawa, O., Ogawa, Y., Miyamoto, Y., Kuwahara, K., Ogawa, E., Igaki, T., Yamashita, J., Masuda, I., *et al.* (1997) *Circulation* **96,** 3737–3744.
19. Ohyama, K., Kawano, H. & Kawamura, K. (1997) *Dev. Brain Res.* **103,** 143–154.
20. Rockman, H. A., Knowlton, K. U., Ross, J., Jr., & Chien, K. R. (1993) *Circulation* **87**, Suppl. VII, VII-14–VII-21.
21. Suda, M., Ogawa, Y., Tanaka, K., Tamura, N., Yasoda, A., Takigawa, T., Uehira, M., Nishimoto, H., Itoh, H., Saito, Y., *et al.* (1998) *Proc. Natl. Acad. Sci. USA* **95,** 2337–2342.
22. Yasoda, A., Ogawa, Y., Suda, M., Tamura, N., Mori, K., Sakuma, Y., Chusho, H., Shiota, K., Tanaka, K. & Nakao, K. (1998) *J. Biol. Chem.* **273,** 11695–11700.
23. Burbach, J. A. (1987) *Am. J. Anat.* **179,** 291–307.
24. John, S. W. M., Krege, J. H., Oliver, P. M., Hagaman, J. R., Hodgin, J. B., Pang, S. C., Flynn, T. G. & Smithies, O. (1995) *Science* **267,** 679–681.
25. Vikstrom, K. L., Bohlmeyer, T., Factor, S. M. & Leinwand, L. A. (1998) *Circ. Res.* **82,** 773–778.
26. Lopez, M. J., Wong, S. K.-F., Kishimoto, I., Dubois, S., Mach, V., Frisen, J., Garbers, D. L. & Beuve, A. (1995) *Nature (London)* **378,** 65–68.
27. Shiota, N., Fukamizu, A., Okunishi, H., Takai, S., Murakami, K. & Miyazaki, M. (1998) *Biochem. J.* **333,** 417–424.
28. Pieruzzi, F., Abassi, Z. A. & Keiser, H. R. (1995) *Circulation* **92,** 3105–3112.
29. Takemoto, M., Egashira, K., Usui, M., Numaguchi, K., Tomita, H., Tsutsui, H., Shimokawa, H., Sueishi, K. & Takeshita, A. (1997) *J. Clin. Invest.* **99,** 278–287.
30. Hama, N., Itoh, H., Shirakami, G., Nakagawa, O., Suga, S., Ogawa, Y., Masuda, I., Nakanishi, K., Yoshimasa, T., Hashimoto, Y., *et al.* (1995) *Circulation* **92,** 1558–1564.
31. Nakagawa, O., Ogawa, Y., Itoh, H., Suga, S., Komatsu, Y., Kishimoto, I., Nishino, K., Yoshimasa, T. & Nakao, K. (1995) *J. Clin. Invest.* **96,** 1280–1287.
32. Oliver, P. M., Fox, J. E., Kim, R., Rockman, H. A., Kim, H.-S., Reddick, R. L., Pandy, K. N., Milgram, S. L., Smithies, O. & Maeda, N. (1997) *Proc. Natl. Acad. Sci. USA* **94,** 14730–14735.